Magnetic and structural analysis of sputtered Co$_{90}$Fe$_{10}$/Au multilayer films for magnetic recording applications

S. CAKMAKTEPE[a], S. DIKEN[b]*

[a]Department of Science Education, Kilis 7 Aralık University, 79000 Kilis, Turkey
[b]Department of Physics, Kilis 7 Aralık University, 79000 Kilis, Turkey

This paper presents the results of investigation on deposition and characterization of cobalt iron (Co$_{90}$Fe$_{10}$) thin films onto gold (Au) underlayers. Co$_{90}$Fe$_{10}$/Au films with different Au underlayer thickness (6, 10, 20, 30 nm) were deposited onto silicon (Si) (100) substrates at room temperature by direct current (DC) magnetron sputtering. Hysteresis curves along hard axis on magneto-optical Kerr effect (MOKE) graphs indicate that 6 nm Au underlayer decreases coercivity (H_c) of Co$_{90}$Fe$_{10}$ film from 37 Oe to 6 Oe. As the remanent magnetization (M_r) decreases, saturation magnetization (M_s) remains relatively high with 6 nm Au underlayer. In addition, grazing-incidence x-ray diffraction (GI-XRD) results confirmed that Co$_{90}$Fe$_{10}$ layer has body-centered cubic (bcc) structure and (110)-oriented texturing. Particle size of the films varied in the range from 107 Å to 46 Å. Furthermore; it is observed that XRD peaks shift towards lower angles with the increasing Au underlayer thickness. Finally, magnetic force microscopy (MFM) images demonstrate dramatic changes in domain structure and confirm MOKE results. These results suggest that Co$_{90}$Fe$_{10}$/Au thin films are promising candidates as write head materials for magnetic recording applications in information technology.

1. Introduction

Recently, innovations and improvements have been increasing drastically in magnetic sensors and data storage technology[1]. Soft magnetic multilayer films play a key role in this progress due to their unique magnetic properties; namely, high saturation magnetization, high magnetic permeability, high Curie temperature and low coercivity[2]–[5]. The most common soft magnetic materials are based on Ni, Fe, Co elements and their binary-ternary combinations produced at different amounts by various techniques[6], [7]. NiFe is the most widely used and extensively investigated soft magnetic pole material for tape and disk heads[8], [9]. However; Co$_{90}$Fe$_{10}$ thin films, as an alternative to NiFe, have been attracting attention for obtaining softer magnetic properties with a suitable underlayer[10]. Perpendicular recording, head density recording heads and spin valves, among others, are prominent application areas of Co$_{90}$Fe$_{10}$ films[11]–[13]. Although low coercivity is required for soft magnetic thin films, coercivity of Co-Fe alloy films prepared by conventional sputtering method ranges from 50 to 100 Oe. Therefore, it is essential to improve a method to obtain Co-Fe alloy films with low coercivity[14]. In recent years, many research have shown that decrease in coercivity of soft magnetic Co-Fe films can be obtained by using different deposition techniques, underlayers and additives. Growing films on different underlayers is a good method to change magnetic properties including coercivity[15], [16]. In our previous study, we investigated magnetic and structural properties

of Co$_{90}$Fe$_{10}$ thin films with four different underlayers (Au, Cu, NiFe and Cr) and our results indicate that Au underlayer reduced the coercive fields significantly thus contributed most to improvement of soft magnetic properties of thin films[17]. However, magnetic and structural properties of Au underlayers with different thickness were not addressed in that study. In this article, we report on magnetic and structural properties of multilayer Co$_{90}$Fe$_{10}$/Au films and investigate changes in depth with respect to Au underlayer thickness.

2. Experimental details

Depositions of Co$_{90}$Fe$_{10}$/Au films were performed on Si (100) substrates at room temperature by DC magnetron sputtering in an ultrahigh vacuum chamber with an ultimate pressure of $1,7 \times 10^{-7}$ Torr. Prior to the deposition, we performed a cleaning process to remove impurities on the surface at 40 W for 40 s. Sputter process was carried out with a 6-tagret system to provide same vacuum pressure for the films. All 40 nm CoFe layers were deposited with a background Ar pressure of 3 mTorr at 300 W dc sputter power. Deposition of Au underlayers (6, 10, 20, 30 nm) were performed at 150 W sputter power and 1 mTorr Ar pressure. The crystallographic phase and crystallite size of all thin films have been determined at room temperature using Grazing Incidence X-ray diffraction (GI-XRD) (Rigaku Ultimate IV) technique in which the diffraction angle is varied in the 2θ= 20–80° range with CuKα radiation. Surface magnetization is

imaged by Magnetic Force Microscopy (MFM) (Park System XE-100) technique in which a non-contact and non-destructive magnetized (perpendicular to the sample plane) tip scans the surface of the films in terms of domain structure. Normalized magnetization hysteresis curves of each film were measured using Magneto-optic Kerr effect (MOKE) magnetometer. Coercivity (H_c) of the films are determined using the hysteresis curves along the hard axis. Remanent magnetization (M_r) and saturation field (M_s) of thin films are also compared.

3. Results and discussion

GIXRD technique is used for a highly accurate crystalline study of very thin films. Average crystallite size was calculated from GI-XRD data with the help of Scherrer equation

$$D = \frac{0.9\lambda}{\beta \cos\theta}$$

where D, λ, θ and β are the crystallite size (nm), wavelength of CuKα radiation (0, 15406 nm), Bragg angle and full width at half-maximum (FWHM) of diffraction peak, respectively. The lattice spacing (d) was calculated using the Bragg diffraction equation[18].

XRD spectra of the monolayer $Co_{90}Fe_{10}$ and multilayer $Co_{90}Fe_{10}$/Au thin films are shown in Fig. 1. Samples exhibited peaks which correspond to (110), (200) reflections for $Co_{90}Fe_{10}$ and (200), (111), (220), (311) reflections for Au. Peaks are well fit to the body-centered cubic (bcc) and face-centered cubic (fcc) crystal lattice structures for CoFe and Au, respectively. All diffraction peaks match well with standard values in JCPDS cards 04-0784 and 49-1567[19], [20]. As clearly seen in Fig.1a monolayer $Co_{90}Fe_{10}$ film shows strong (110) and weak (220) peaks. It is observed from Fig1.b that 6 nm Au underlayer affected the crystal structure of $Co_{90}Fe_{10}$ film by eliminating CoFe (110) peak however weak CoFe (200), Au (220) peaks are observed. This implies that 6 nm

underlayer changes the preferred orientation of $Co_{90}Fe_{10}$ thin film from (110) to (200). Fig.1c shows the effect of 10 nm Au underlayer; peak intensity of Au (111), Au (200), CoFe (110) reflections are stronger and peaks are relatively broadened. Broadening of the diffraction peaks implies smaller grain size. In Fig1.d and Fig1.e intensity of the peaks decreased but texture remained. Similar structural results are also reported by Kim et al.[21] and Yoon et al[22]. In addition, it is also found that diffraction peaks shift towards lower angle with the increasing Au underlayer thickness. The shift reaches a maximum value when the thickness of Au underlayer is 30 nm. Shift of the peaks to lower angles can be attributed to compressive strain, distortions in the host lattices, increasing lattice parameter (a) and lattice spacing (d)[23]-[27].
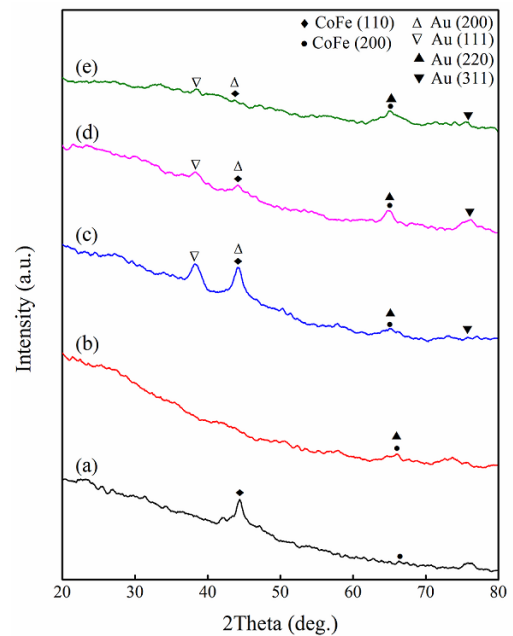

Fig.1 GI-XRD diffraction patterns of (a) monolayer (40 nm) $Co_{90}Fe_{10}$ and multilayer (40 nm) $Co_{90}Fe_{10}$ films with (b) (6 nm), (c) (10 nm), (d) (20 nm), (e) (30 nm) Au underlayers.

Table 1. The calculated average crystallite size (D), full width at half maximum (FWHM), lattice spacing (d), lattice parameter (a) and angle of diffraction of the films.

Sample	D (Å)	FWHM	d (Å)	a (Å)	2θ (°) [110]
40 nm $Co_{90}Fe_{10}$	107,27	0,800	2,037	2,880	44,44
40 nm $Co_{90}Fe_{10}$ / 6 nm Au	-	-	-	-	-
40 nm $Co_{90}Fe_{10}$ / 10 nm Au	72,55	1,182	2,047	2,894	44,22
40 nm $Co_{90}Fe_{10}$ / 20 nm Au	69,83	1,228	2,047	2,894	44,22
40 nm $Co_{90}Fe_{10}$ / 30 nm Au	46,08	1,857	2,072	2,930	43,65

In order to obtain more structural information, crystallographic parameters of each sample were calculated and results are shown on Table.1. According to these results, Au underlayer thickness influences the particle size, i.e., as the Au underlayer thickness increases; particle size decreases, lattice constant (a) and lattice spacing (d) increase. All of the results obtained from XRD measurements confirm that the structural properties of the

$Co_{90}Fe_{10}$ thin films have been strongly correlated to Au underlayer thickness.

Magnetic behavior of the films was investigated by a magneto-optic Kerr effect magnetometer (MOKE). Fig 2 shows MOKE hysteresis curves for $Co_{90}Fe_{10}$ films with different Au underlayer thickness at room temperature. Monolayer $Co_{90}Fe_{10}$ film exhibits a hard axis coercivity of 37 Oe. As we continue to investigate Fig 2, it is seen that

coercivity is reduced significantly to 4,6 Oe by employing 6 nm Au underlayer. Thus, $Co_{90}Fe_{10}$/Au film is found to have a soft magnetic characteristic. Furthermore coercivity is reduced from 37 Oe to 16 Oe, 7,5 Oe and 13,3 Oe, respectively by employing 10, 20 and 30 nm Au underlayers to monolayer $Co_{90}Fe_{10}$. High saturation magnetization and low remanent magnetization are required for write head materials besides low coercivity.

Through the comparison of the MOKE results, it is deduced that 6 nm Au underlayer decreases hard axis remanent magnetization (M_r) of $Co_{90}Fe_{10}$ while saturation magnetization (M_s) is still relatively high. It is observed from the MOKE curves that all films are sensitive to underlayer thickness and show ferromagnetic behavior. These results are also supported by MFM images.
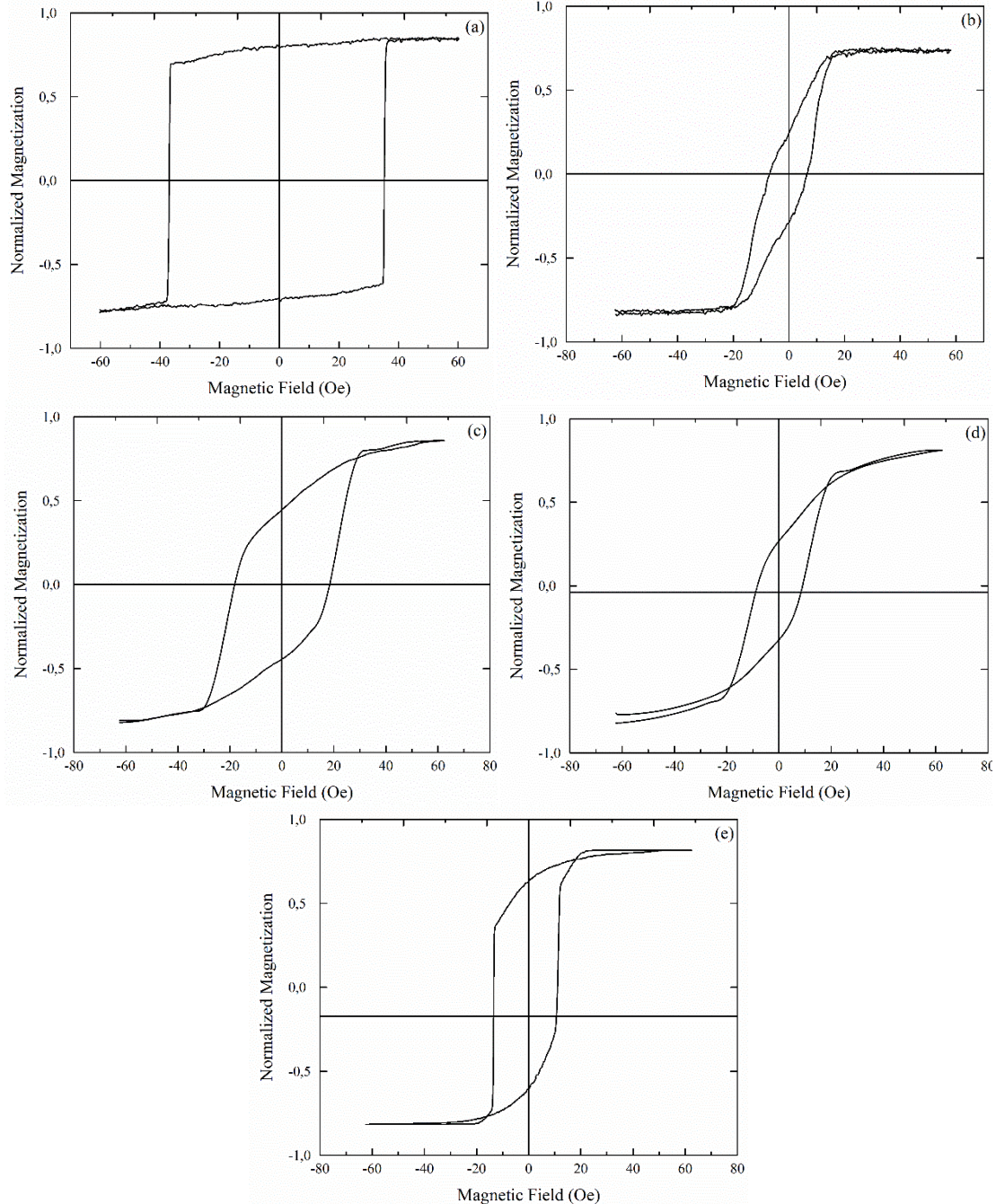

Fig.2. Hard axis MOKE hysteresis curves of (a) monolayer (40 nm) $Co_{90}Fe_{10}$ and multilayer (40 nm) $Co_{90}Fe_{10}$ films with (b) (6 nm), (c) (10 nm), (d) (20 nm), (e) (30 nm) Au underlayers.

MFM images of films for (5×5) μm^2 scan size are presented in Fig 3 where dark and bright areas correspond to domains of opposite magnetization. Ripple like domain structure which corresponds to a higher coercivity, in

comparison to other films, can be seen in Fig 3a and Fig 3c. Moreover, considerably smaller magnetic domains are observed in Fig 3b, Fig 3d and Fig 3e. Decrease in coercivity values due to the different underlayer thickness

explains the variations in domain structures. These results are also consistent with MOKE measurements and the
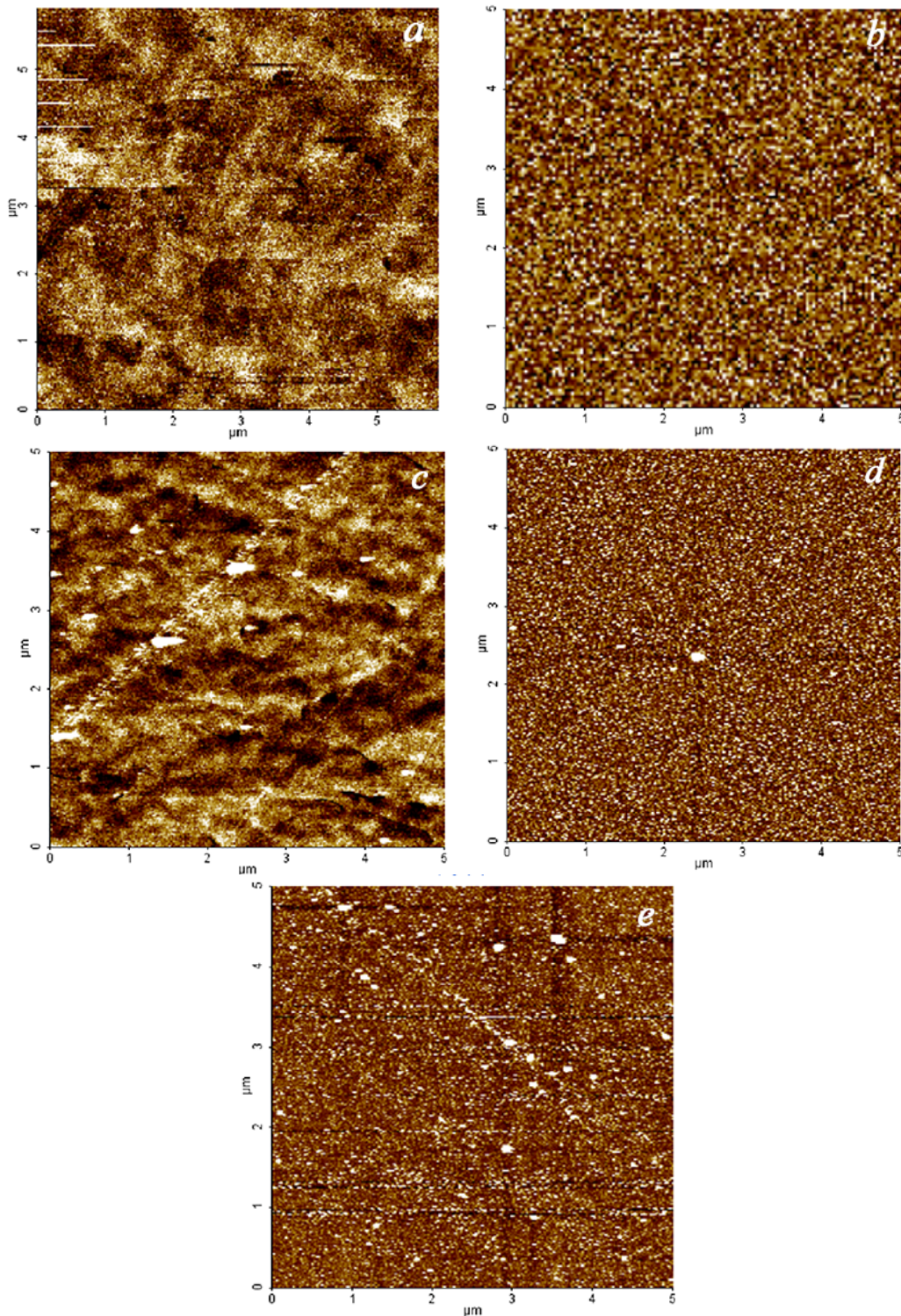
previous report by Cakmaktepe[17].

Fig.3 MFM images of (a) monolayer (40 nm) $Co_{90}Fe_{10}$ and multilayer (40 nm) $Co_{90}Fe_{10}$ films with (b) (6 nm), (c) (10 nm), (d) (20 nm), (e) (30 nm) Au underlayers.

4. Conclusion

However it is a very complex challenge to create new soft magnetic materials for magnetic recording applications, we successfully deposited, investigated and

characterized $Co_{90}Fe_{10}$ films on Au underlayers with four different thicknesses ranging from 6 nm to 30 nm. Films deposited on 6nm Au underlayer showed the highest decrease in coercivity (H_c) by 4,6 Oe beside lowest remanent magnetization (M_r) and relatively high saturation

magnetization (M_s) thus the CoFe/Au film gained soft magnetic character. Moreover, experimental results indicate that particle size and preferred orientation of $Co_{90}Fe_{10}$/Au thin films are depended on Au underlayer thickness. As a conclusion, the authors have shown a new method of controlling the characteristics of sputtered $Co_{90}Fe_{10}$ thin films for magnetic recording applications by applying Au underlayer with different thickness. Further studies are in progress to understand the effects of Au underlayer on electrical properties of $Co_{90}Fe_{10}$ thin films.

References

[1] S. X. Wang, A. M. Taratorin, Magnetic Information Storage Technology, Academic Press, London, 1999.
[2] G. E. Fish, Proc. IEEE, **78**, 6, 947 (1990).
[3] Arrott, A.S., J. Magn. Magn. Mater., **215–216**, 6 (2000).
[4] G. Herzer, J. Magn. Magn. Mater., **157–158**, 133 (1996).
[5] Y. T. Chen, S. U. Jen, Y. D. Yao, J. M. Wu, G. H. Hwang, T. L. Tsai, Y. C. Chang, A. C. Sun, J. Magn. Magn. Mater., **304**,1, e71 (2006).
[6] T. Sahin, H. Kockar, M. Alper, J. Magn. Magn. Mater., **373**, 128 (2015).
[7] E. Klokholm ,J. A. Aboaf, J. Appl. Phys., **52**(3), 2474 (1981).
[8] S. T. Patton and B. Bhushan, Wear, **202**, 1, 99–109 (1996).
[9] W. D. Doyle, J. Appl. Phys., **38**(3), 1441 (1967).
[10] A. Caruana Finkel, N. Reeves-McLaren, N. A. Morley, J. Magn. Magn. Mater., **357**, 87 (2014).
[11] F. Karnbach, M. Uhlemann, A. Gebert, J. Eckert, K. Tschulik, Electrochim. Acta, **123**, 477 (2014).
[12] C. L. Platt, A. E. Berkowitz, D. J. Smith, M. R. McCartney, J. Appl. Phys., **88(**4), 2058 (2000).
[13] T. Osaka, M. Takai, K. Hayashi, K. Ohashi, M. Saito, K. Yamada, **392**(6678), 796 (1998).
[14] M. Vopsaroiu, M. Georgieva, P. J. Grundy, G. Vallejo Fernandez, S. Manzoor, M. J. Thwaites, K. O'Grady, J. Appl. Phys., **97**(10), 10N303 (2005).
[15] X. Wang, F. Zheng, Z. Liu, X. Liu, D. Wei, F. Wei, J. Appl. Phys., **105**(7), 07B714 (2009).
[16] K. K. M. Pandey, J. S. Chen, B. C. Lim, G. M. Chow, J. Appl. Phys., **10 (**7), 073904 (2008).
[17] S. Cakmaktepe, M. I. Coskun, and A. Yildiz, Lith. J. Phys., **53**, 2 (2013).
[18] B. D. Cullity, S. R. Stock, Elements of X-Ray Diffraction 3rd ed. Prentice Hall, 2001.
[19] G. Pookat, H. Thomas, S. Thomas, S. H. Al-Harthi, L. Raghavan, I. A. Al-Omari, D. Sakthikumar, R. V. Ramanujan,, M. R. Anantharaman, Surf. Coatings Technol., **236**, 246 (2013).
[20] W. B. Zhao, J. J. Zhu, H. Y. Chen, J. Cryst. Growth, **258**(1–2), 176 (2003).
[21] B. G. Kim, S. J. Yoon, I. T. Jeon, K. H. Kim, J. H. Wu, Y. K. Kim, IEEE Trans. Magn., **48**(11), 3929 (2012).
[22] S. J. Yoon, B. G. Kim, I. T. Jeon, J. H. Wu, Y. K. Kim, Appl. Phys. Express, **5**(10), 103003 (2012).
[23] Dantas, N. O., et al., Journal of Non-Crystalline Solids **354**, 4827 (2008).
[24] Sönmezoğlu, S., Akman, E., Applied Surface Science **318**, 319 (2014).
[25] B. Avar, M. Gogebakan, S. Ozcan, S. Kerli, Journal of the Korean Physical Society **65.5**, 664 (2014).
[26] Li, Wei, et al., Materials Letters **65.4**, 636 (2011).
[27] Valant, Matjaz, et al., J. Optoelectron. Adv. Mater. **9**(5), 1377 (2007).

_____
* Corresponding author: sinandiken@hotmail.com
                          sinandiken@kilis.edu.tr